ANS-LHS

OPEN ACCESS

Advanced Natural Sciences: Life and Health Sciences,
ISSN: 3107-636X, Vol-3, Issue-2,
July-Dec, 2026, 333-350
https://www.indjournals.com

Research Article

Thalamocortical morphometric patterns in idiopathic generalized and mesial temporal lobe epilepsy: findings from 1.5 T MRI cortical thickness and volumetry

Running title: Thalamocortical morphometry in epilepsy

Dr Archit Tyagi[1,*] and Dr Shino Shajan[2]

[1]Assistant Professor, Department of Radiodiagnosis, Subharti Medical College, Meerut, Uttar Pradesh, India. https://orcid.org/0009-0005-3332-2174

[2]Assistant Professor in Radiology, SUT Medical College, Trivandrum, Kerala, India. sitet2005@gmail.com

Article Info:

***Corresponding author**
Dr Archit Tyagi
Assistant Professor, Department of Radiodiagnosis, Subharti Medical College, Meerut, Uttar Pradesh, India.
archittyagi90@gmail.com

DOI:10.68819/anslhs.2026.0039

[Received 11-10-2026,
Accepted 09-11-2026,
Published 11-11-2026]

Publishers Note: Natural Science Association stays neutral with regard to jurisdictional claims in published maps and institutional affiliations.

Copyright: ©2026 by the author(s). This is an Open Access article distributed under the terms of the Creative Commons Attribution 4.0 license (unless stated otherwise) permits unrestricted use, distribution, and reproduction in any medium, provided the original work is properly cited.
https://creativecommons.org/licenses/by/4.0//

Abstract

Background: Structural differences in epilepsy may involve distributed cortico-subcortical networks beyond the apparent seizure onset region. Quantitative descriptions from routine 1.5 T MRI examinations in South Asian clinical populations remain limited.

Objective: To describe regional cortical thickness and subcortical volume deviations in idiopathic generalized epilepsy (IGE) and mesial temporal lobe epilepsy (MTLE) on 1.5 T MRI and explore whether similar descriptive patterns occur across clinical subgroups.

Methods: This retrospective cross-sectional study included 100 patients with epilepsy (age 5–72 years; 57 male) imaged between January and June 2019 using a 1.5 T Siemens Magnetom Essenza system. Automated CAT12 analysis of three-dimensional T1 datasets was performed for 60 patients with IGE and 20 with MTLE (11 right-sided and 9 left-sided). Regional cortical thickness and thalamic and hippocampal volumes were compared descriptively with fixed region-specific reference means; 20 patients with other structural lesions were characterized etiologically but did not undergo morphometry. No matched healthy control group or formal inferential comparison was available.

Results: Across five analytic subgroups, the reported reference-based deviations included bilateral precentral cortical thinning (−6.0% to −10.8%) and reduced left thalamic volume (−4.9% to −10.2%). The MTLE subgroups generally had numerically larger deviations and showed ipsilateral hippocampal volume reduction (−14.4% in right MTLE; −14.0% in left MTLE) and bilateral transverse temporal gyrus thinning (−6.4% to −6.9%). Insular and postcentral cortical thickness exceeded the reference means in both sex-defined IGE groups, with larger percentage deviations in the female-defined group. The paediatric and sex-defined IGE subgroups overlapped, and no independent between-group statistical comparison was undertaken.

Conclusions: Similar precentral and left-thalamic reference-based deviations were observed across IGE and MTLE subgroups on automated 1.5 T morphometry. These single-centre descriptive findings are hypothesis-generating because subgroup sizes were small, the IGE strata were partly overlapping and the reference means were not locally matched. Clinical diagnostic, prognostic and risk-stratification applications require independent validation.

Keywords: epilepsy; cortical thickness; subcortical volume; thalamus; precentral gyrus; insula; CAT12; idiopathic generalized epilepsy; mesial temporal lobe epilepsy; magnetic resonance imaging.

1. Introduction

Epilepsy is one of the most common chronic neurological disorders worldwide, affecting approximately 0.6–1.5% of the population and comprising many different syndromes and conditions [1,2]. Although most patients respond to antiepileptic drug therapy, roughly one third remain pharmacoresistant, and alternative treatments such as resective surgery or neurostimulation are not always appropriate or effective [3]. For this large subgroup, a biologically meaningful characterization of the epileptogenic network is a prerequisite for precision therapy, yet the underlying disease biology remains unexplained for most cases of the common epilepsies.

Over the past two decades the conceptualization of epilepsy has progressively shifted from a strictly focal model towards a network disorder, in which structural and functional injury is distributed across interconnected cortico-subcortical circuits [4]. Convergent evidence shows that even "MRI-negative" temporal lobe epilepsy behaves as a network disorder of neocortical connectivity [5]. Hippocampal sclerosis remains the commonest pathological substrate of mesial temporal lobe epilepsy (MTLE) [6], but extrahippocampal abnormalities particularly in the thalamus and neocortex are frequently observed and increasingly regarded as part of the disease itself rather than an epiphenomenon [4,5].

At the syndrome level, the Enhancing Neuro Imaging Genetics through Meta-Analysis (ENIGMA)-Epilepsy consortium demonstrated distributed structural differences across common epilepsy groups, including bilateral precentral cortical thinning and a reduction in right thalamic volume relative to healthy controls [7]. Earlier single-centre investigations described structural abnormalities in both left- and right-sided MTLE [8] and laterality-dependent differences in large-scale cerebral networks [9]. These case-control findings provide a reference for anatomical comparison, although their effect sizes cannot be directly equated with percentage deviations from a separate normative dataset. Idiopathic generalized epilepsy (IGE), a clinically and biologically distinct group typically associated with a "normal" MRI on clinical inspection, is nonetheless accompanied by quantifiable structural change. Quantitative MRI has demonstrated widespread cerebral structural changes in IGE since the late 1990s [10], and dedicated volumetric studies have confirmed structural abnormalities at the group level [11]. The thalamus has emerged as a central node in this network: thalamic volumes are reduced across temporal, extratemporal and idiopathic generalized epilepsies [12], regional atrophy of the basal ganglia and thalamus is demonstrable in IGE [13], and MRI-based morphometric correlation analysis has delineated a thalamo-cortical network pathology in IGE [14]. These observations resonate with the "system epilepsies" hypothesis, which proposes that a broad range of epilepsies share vulnerability within distributed, hierarchically organized networks prominently the thalamo-cortical system [15].

Three practical questions remain. First, it is useful to describe the anatomical patterns obtained by automated morphometry from routine 1.5 T examinations, despite potential differences in acquisition and normative reference populations. Second, ranking regional deviations against a fixed reference mean provides a descriptive summary but does not establish that a patient is abnormal without an appropriately matched comparison group. Third, apparent variation by age, sex and epilepsy syndrome requires cautious interpretation when clinical strata are small or overlapping.The objectives of this single-centre retrospective study were to quantify regional cortical thickness and thalamic and hippocampal volumes using CAT12 on 1.5 T MRI; describe patterns of reference-based deviation in IGE and right- and left-sided MTLE; summarize the distribution of differences in paediatric and sex-defined IGE subgroups; and identify regions suitable for confirmation in controlled longitudinal studies.

2. Materials and methods

2.1 Study design and setting

This was a retrospective, cross-sectional, single-centre study of brain MRI records of patients with epilepsy referred to the radiology department and imaged at the Atmajyoti MRI Centre, New Civil Hospital. All examinations performed between 1 January 2019 and 1 June 2019 were considered. The study was conducted in accordance with the Declaration of Helsinki and applicable institutional requirements.

2.2 Participants

During the study period, 120 epilepsy MRI records were screened. Twenty were excluded because of progressive neurological disease, including Rasmussen encephalitis, or previous epilepsy surgery. The remaining 100 records formed the study cohort.

Eligible examinations were obtained from children and adults referred for MRI because of clinically diagnosed epilepsy, including generalized seizures, focal seizures with or without secondary generalization, MTLE and epilepsy associated with demonstrable structural lesions or previous neurological insults (including trauma or cerebrovascular events). Patients with either focal or generalized epilepsy could be included regardless of whether structural abnormalities were identified on conventional MRI. Progressive neurological disease and previous epilepsy surgery were exclusion criteria; drug resistance was not an eligibility requirement for every diagnostic group.

Clinical information recorded at the time of imaging, including presenting seizure characteristics, previous medical history, family history and relevant neurological or neurodevelopmental conditions, was reviewed. The clinical and imaging information used for analysis was de-identified.

2.3 MRI acquisition

All imaging was performed on a 1.5 Tesla scanner (Siemens Magnetom Essenza) with protocols tailored to patient age (Table 1). Every acquisition began with a three-plane localizer. The adult protocol comprised axial T2 turbo spin-echo (TSE), axial T2 fluid-attenuated inversion recovery (FLAIR), coronal T1 spin-echo, sagittal T2 TSE, and high-resolution (2 mm) oblique-coronal T2 and T1 TSE slices planned perpendicular to the long axis of the hippocampus, followed by a three-dimensional (3D) isotropic T1-weighted MPRAGE or VIBE acquisition. The paediatric protocol comprised T2/proton-density dual-echo axial (3 mm, small field of view), T1 TSE axial (3 mm), FLAIR coronal (3 mm), T1 TSE sagittal (3 mm) and diffusion-weighted imaging (4 mm), followed by a 3D T1 MPRAGE (1 mm isotropic) reformatted in the coronal-oblique plane perpendicular to the hippocampus. The oblique-coronal planes were angled to avoid partial-volume effects at the mesial temporal structures, and voxel dimensions were chosen to permit cortical segmentation and hippocampal volumetry.

Table 1. Standardized epilepsy MRI acquisition protocol (Siemens Magnetom Essenza, 1.5 T).

Sequence	Adult protocol	Paediatric protocol
Localizer	Three-plane localizer (< 25 s) to plan all sequences	Three-plane localizer
T2 TSE	Axial; whole brain from vertex to foramen magnum, angled perpendicular to the 3rd-ventricle/brainstem axis	T2 + proton-density dual echo, axial, small field of view, 3 mm
T2 FLAIR	Axial; angled parallel to the genu–splenium axis of the corpus callosum	Coronal, small field of view, 3 mm
T1 SE / TSE	Coronal; planned parallel to the brainstem	T1 TSE axial (3 mm) and T1 TSE sagittal (3 mm), small field of view
Oblique coronal T2 + T1 TSE	2 mm high-resolution slices, perpendicular to the long axis of the hippocampus, covering both temporal lobes	Covered by 3D MPRAGE coronal-oblique reformats
DWI	—	EPI trace axial, small field of view, 4 mm
3D T1 (MPRAGE / VIBE)	3D isotropic T1-weighted MPRAGE or VIBE	3D T1 MPRAGE, 1 mm isotropic; coronal-oblique reformats perpendicular to the hippocampus (nasion to inion)

2.4 Image post-processing

Structural 3D T1 datasets were post-processed with the Computational Anatomy Toolbox (CAT12) running under SPM12. Pre-processing included spatial registration to a common

stereotactic space, intensity non-uniformity correction, tissue segmentation and parcellation. Cortical thickness was estimated with the surface-based projection-based thickness (PBT) algorithm, in which topology correction, spherical mapping and spherical registration are performed in a single processing step, providing both hemispheric surface reconstruction and voxelwise thickness estimation. Regional measures were then extracted using region-based morphometry: volumetric and surface atlases of predefined regions of interest were mapped onto each individual brain through high-dimensional spatial registration, yielding mean cortical thickness for each labelled gyrus and volume measures for subcortical nuclei, following the automated gyral labelling strategy described by Desikan and colleagues [16].

Each processed dataset underwent visual quality assessment for segmentation errors, with reprocessing when required. Regional cortical thickness and subcortical volume summaries were compared with the reference means tabulated for the CAT12-based analysis. The same reference mean for each anatomical region was applied to all analytic subgroups; these reference comparisons were not individually standardized for patient age, sex, local population or scanner. Regional percentage deviations therefore represent descriptive differences from the selected reference values rather than validated measures of patient-level abnormality.

2.5 Study groups and subgroups

The cohort comprised patients with IGE (n = 60), right-sided MTLE (n = 11), left-sided MTLE (n = 9) and other structural or symptomatic epilepsies (n = 20). The structural group included infarction, central nervous system infection, cystic encephalomalacia, tumour, vascular or developmental malformation and haemorrhage. CAT12-based cortical thickness and subcortical volume measurements were available for the 80 patients with IGE or MTLE. The remaining 20 patients contributed only to the descriptive clinical and etiological distribution and were not used as a morphometric control group.

Within IGE, a paediatric subgroup younger than 18 years comprised 30 patients of both sexes, while the sex-defined summaries included 32 male and 28 female patients across the age range. Paediatric patients therefore contributed both to the age-defined subgroup and to one of the two sex-defined groups. These partially overlapping strata were not independent samples, and their numerical differences were not interpreted as independent age or sex effects.

2.6 Outcome measures

For each hemisphere, cortical thickness was extracted for the medial temporal cortex; the superior, middle, inferior and transverse (Heschl) temporal gyri; frontal, parietal and occipital cortical regions; the insula; cingulate cortex; and precentral and postcentral gyri. Thalamic and hippocampal volumes were obtained bilaterally. For every region, the percentage deviation of the patient subgroup mean from the corresponding reference mean was calculated as follows:

% deviation = (patient group mean − reference mean) / reference mean × 100.

A negative deviation indicates a subgroup mean below its selected reference mean, and a positive deviation indicates a subgroup mean above it. These signs describe the direction of the comparison; without matched controls, they do not in themselves establish pathological atrophy, hypertrophy or a clinically significant abnormality. Regions were ranked by the absolute magnitude of the descriptive deviation.

2.7 Statistical analysis

Analysis was descriptive because of the small MTLE groups, partial overlap among IGE strata and absence of an in-house control cohort. Continuous summaries are presented as mean ± standard deviation (SD), and regional differences are expressed as percentages relative to a fixed region-specific reference mean. No independent between-group hypothesis tests, multiple-comparison-adjusted analyses or patient-level predictive models were performed. Confidence intervals for reference-based deviations were not estimated because patient-level measurements and the sampling characteristics of the comparator reference data were unavailable; intervals derived from the

displayed rounded summaries would not capture this uncertainty. Differences in deviation magnitude were treated as exploratory observations and not as evidence of statistically significant group effects.

2.8 Ethics

The study used fully anonymized, retrospectively acquired clinical records; no identifiable patient data were processed. Individual informed consent was waived by the institutional ethics committee, which approved the retrospective analysis.

3. Results

3.1 Cohort characteristics

MRI images of a total of 100 patients were evaluated retrospectively from the stored database (Figure 1). Patients ranged in age from 5 to 72 years (Table 2). The largest age band was 5–15 years (38 patients, 38.0%), followed by 27–37 years (21, 21.0%) and 38–48 years (16, 16.0%); 9 patients (9.0%) were 16–26 years, 7 (7.0%) were 49–59 years, 5 (5.0%) were 60–70 years and 4 (4.0%) were older than 70 years. Fifty-seven patients (57.0%) were male and 43 (43.0%) female; the male predominance was most marked in the youngest band (24 of 38 patients below 16 years were male) and reversed in the 16–26-year band (Table 2).

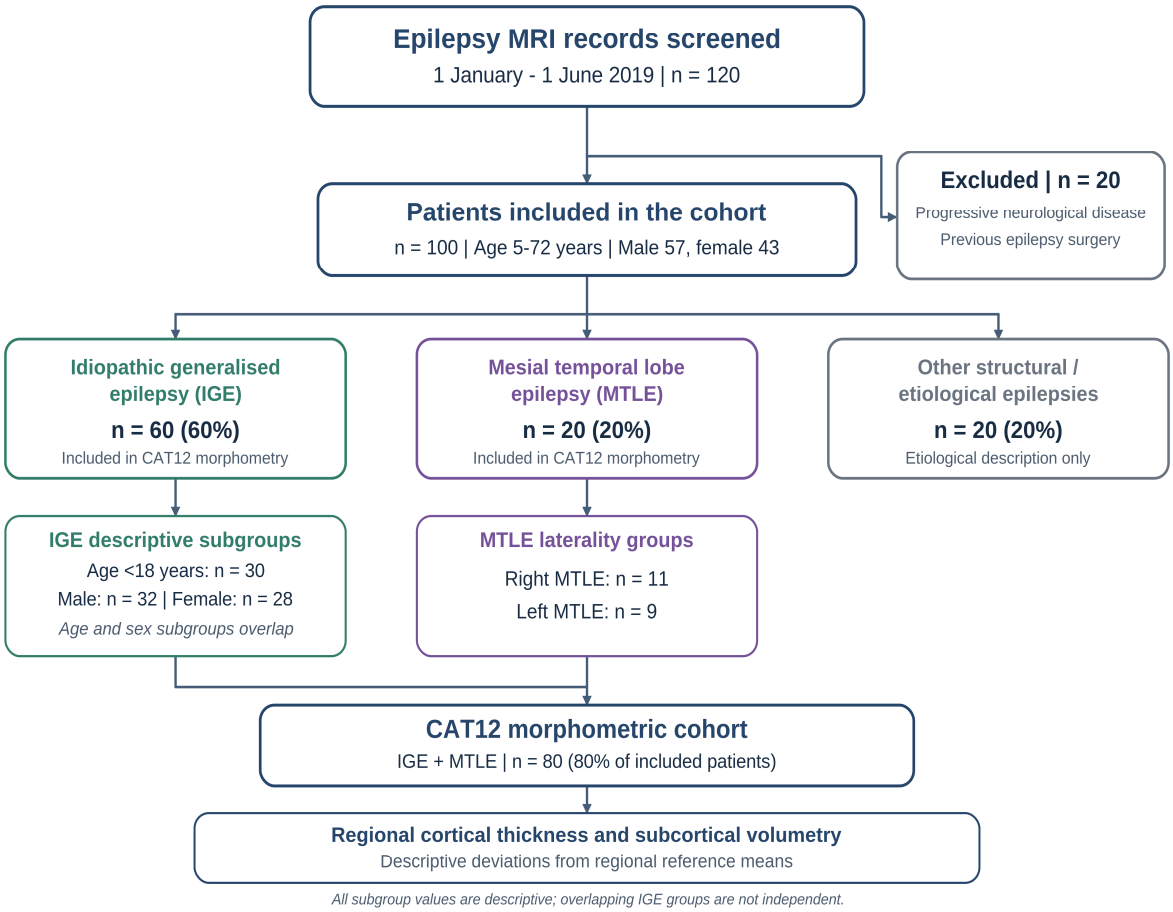


Figure 1. Study flow and analytic-group allocation. Among 120 epilepsy MRI records screened from 1 January to 1 June 2019, 20 were excluded because of progressive neurological disease or previous epilepsy surgery. The remaining 100 patients comprised idiopathic generalised epilepsy (IGE; n = 60), mesial temporal lobe epilepsy (MTLE; right n = 11, left n = 9) and other structural or etiological epilepsies (n = 20). Automated CAT12 morphometry was performed only for the IGE and MTLE groups (total n = 80); the other 20 patients contributed to the descriptive etiological profile. The IGE subgroup aged <18 years (n = 30) overlaps the sex-defined subgroups (male n = 32; female n = 28), and their sample sizes are therefore not additive.

Table 2. Demographic, clinical and etiological profile of the cohort (n = 100). Panel A: age and sex; Panel B: recorded seizure-type categories; Panel C: diagnostic groups; Panel D: etiologies in the other structural group. GTCS: generalized tonic–clonic seizure category not further subdivided in the summary; SGTCS: secondarily generalized tonic–clonic seizures; PGTCS: primary generalized tonic–clonic seizures; SPS/CPS: simple/complex partial seizures; AB: absence; MY: myoclonic seizures. Recorded seizure categories should not be equated directly with syndrome classification.

Characteristic	n	%
A. Age and sex distribution (years)		
5–15 (M/F)	38 (24/14)	38.0
16–26 (M/F)	9 (4/5)	9.0
27–37 (M/F)	21 (11/10)	21.0
38–48 (M/F)	16 (7/9)	16.0
49–59 (M/F)	7 (4/3)	7.0
60–70 (M/F)	5 (4/1)	5.0
>70 (M/F)	4 (3/1)	4.0
Total	100 (57 M / 43 F)	100.0
B. Clinical seizure type		
GTCS — generalized tonic–clonic (category not further specified)	38	38.0
SGTCS — secondarily generalized tonic–clonic	21	21.0
SPS — simple partial seizures	12	12.0
CPS — complex partial seizures	12	12.0
PGTCS — primary generalized tonic–clonic	10	10.0
AB — absence seizures	4	4.0
MY — myoclonic seizures	3	3.0
C. Syndrome group		
IGE (idiopathic generalized epilepsy)	60	60.0
MTLE (right 11; left 9)	20	20.0
Others — structural, non-idiopathic	20	20.0
D. Etiology of the Others group		
CNS infection (I)	6	30.0
Acute infarct (AI)	3	15.0
Cystic encephalomalacia (CE)	3	15.0
Chronic infarct (CI)	3	15.0
Tumour (T)	2	10.0
Developmental malformation (DM)	1	5.0
Haemorrhage (H)	1	5.0
Vascular malformation (VM)	1	5.0

The recorded seizure-type categories are shown in Table 2. Generalized tonic–clonic seizures (GTCS category, 38 patients; 38.0%) were the most frequent label, followed by secondarily generalized tonic–clonic seizures (21; 21.0%), simple and complex partial seizures (12 each; 12.0% each), primary generalized tonic–clonic seizures (10; 10.0%), absence seizures (4; 4.0%) and myoclonic seizures (3; 3.0%). These are the mutually exclusive categories used in the clinical summary, although their terminology has conceptual overlap. By syndrome group, 60 patients (60.0%) were classified as IGE, 20 (20.0%) as MTLE (11 right-sided, 9 left-sided) and 20 (20.0%) as the non-idiopathic Others group (Table 2). Thus, 80% of the cohort comprised the two syndromes subjected to morphometric analysis.

Within the Others group, central nervous system infection accounted for 6 of 20 cases (30.0%). Acute infarction, cystic encephalomalacia and chronic infarction each accounted for 3 cases (15.0%), together representing 9 of 20 patients (45.0%) in this group. Tumours accounted for 2 cases (10.0%), and developmental malformation, haemorrhage and vascular malformation for 1 case (5.0%) each. The distribution of structural etiologies by age was descriptive and was not subjected to statistical comparison.

3.2 IGE group — paediatric subgroup (< 18 years, n = 30)

In the paediatric IGE subgroup, the largest negative cortical deviations involved the precentral gyri (Table 3, Panel A). Mean right and left precentral thicknesses were 2.34 ± 0.03 mm and 2.35 ± 0.03 mm, respectively, compared with reference means of 2.50 mm on each side (−6.4% and −6.0%). Left thalamic volume was 8.15 ± 0.07 against a reference mean of 8.57 (−4.9%), while right thalamic volume was 8.38 ± 0.12 versus 8.04 (+4.2%). Hippocampal mean volumes were close to the selected reference means (right +2.5%, left 0.0%). These results describe relative deviations within this subgroup; they do not establish a causal or age-specific pattern.

Elsewhere the deviations were subtle: medial temporal thickness was reduced on the right (−3.2%) but preserved on the left (−0.4%); lateral temporal gyri showed mild bilateral thinning (superior −1.4%/−1.1%, middle −1.1%/−1.1%, inferior −1.4%/−1.8%, transverse −3.5%/−2.8%, right/left); frontal thinning was mild (−1.2% right, −2.7% left); parietal and occipital lobes were essentially normal; insular cortex was mildly thickened bilaterally (+2.3% right, +1.0% left); and the cingulate gyri were symmetric (−2.0% right, +0.8% left). Postcentral thickness was unchanged (+0.5% bilaterally).

The paediatric IGE results were summarized for the combined age-defined group (n = 30). Separate denominators and complete regional estimates by seizure semiology were not available for a quantitative comparison within this subgroup.

3.3 IGE group — sex subgroups

Male IGE subgroup (n = 32). This subgroup had positive reference-based differences in insular and cingulate thickness and negative differences in precentral thickness and left thalamic volume (Table 3, Panel B). Bilateral insular thickness was 3.24 ± 0.21 mm on the right and 3.22 ± 0.20 mm on the left, compared with reference means of 3.05 mm (+6.2% and +5.6%). Cingulate thickness differed by +2.4% bilaterally. The right and left precentral deviations were −8.0% and −7.6%, and postcentral deviations were +4.4% and +3.9%. Left thalamic volume differed by −8.2%, whereas the right thalamic and hippocampal means were close to reference values. Additional cortical differences were generally smaller. This subgroup included paediatric male patients and was not independent of the paediatric summary.

Female IGE subgroup (n = 28). The largest positive reference-based differences were observed in the postcentral cortex (+9.7% bilaterally) and insula (+8.2% right and +7.5% left) (Table 3, Panel C). Bilateral precentral thickness was below the reference means (−8.4% right and −8.0% left), as was left thalamic volume (−8.2%). Left frontal thickness differed by −4.7%, whereas right frontal thickness was close to the selected reference mean (−0.4%). Hippocampal mean volumes were close to reference values. These descriptive percentages were numerically larger than several corresponding male subgroup values but cannot establish sex-related effects because age distribution and other potential confounders were not adjusted.

Table 3. Cortical thickness and subcortical volume summaries in IGE. Panel A: paediatric participants aged <18 years (n = 30); Panel B: male participants across ages (n = 32); Panel C: female participants across ages (n = 28). Paediatric participants also occur in the corresponding sex-defined panel. Percentage deviations compare subgroup means with the same fixed region-specific reference means in all panels and are descriptive rather than age- or sex-standardized.

Region	Patient value (mean ± SD)	Reference value (mean ± SD)	Difference	Deviation (%)
Panel A. IGE — paediatric (< 18 years), both sexes (n = 30)				
Medial temporal (R)	2.69 ± 0.08	2.78 ± 0.12	-0.09	-3.2
Medial temporal (L)	2.77 ± 0.04	2.78 ± 0.12	-0.01	-0.4
Lateral temporal – STG				
STG (R)	2.78 ± 0.04	2.82 ± 0.09	-0.04	-1.4
STG (L)	2.79 ± 0.04	2.82 ± 0.09	-0.03	-1.1
Lateral temporal – MTG				
MTG (R)	2.79 ± 0.03	2.82 ± 0.09	-0.03	-1.1
MTG (L)	2.79 ± 0.03	2.82 ± 0.09	-0.03	-1.1
Lateral temporal – ITG				

ITG (R)	2.78 ± 0.03	2.82 ± 0.09	-0.04	-1.4
ITG (L)	2.77 ± 0.03	2.82 ± 0.09	-0.05	-1.8
Lateral temporal – TTG (Heschl)				
TTG (Heschl) (R)	2.72 ± 0.03	2.82 ± 0.09	-0.10	-3.5
TTG (Heschl) (L)	2.74 ± 0.04	2.82 ± 0.09	-0.08	-2.8
Frontal lobe				
Frontal lobe (R)	2.54 ± 0.04	2.57 ± 0.12	-0.03	-1.2
Frontal lobe (L)	2.50 ± 0.08	2.57 ± 0.12	-0.07	-2.7
Parietal lobe				
Parietal lobe (R)	2.25 ± 0.03	2.25 ± 0.12	+0.00	+0.0
Parietal lobe (L)	2.26 ± 0.03	2.25 ± 0.12	+0.01	+0.4
Occipital lobe				
Occipital lobe (R)	1.85 ± 0.04	1.84 ± 0.10	+0.01	+0.5
Occipital lobe (L)	1.86 ± 0.03	1.84 ± 0.10	+0.02	+1.1
Insular cortex				
Insular cortex (R)	3.12 ± 0.14	3.05 ± 0.17	+0.07	+2.3
Insular cortex (L)	3.08 ± 0.09	3.05 ± 0.17	+0.03	+1.0
Cingulate gyrus				
Cingulate gyrus (R)	2.49 ± 0.10	2.54 ± 0.12	-0.05	-2.0
Cingulate gyrus (L)	2.56 ± 0.03	2.54 ± 0.12	+0.02	+0.8
Precentral gyrus				
Precentral gyrus (R)	2.34 ± 0.03	2.50 ± 0.05	-0.16	-6.4
Precentral gyrus (L)	2.35 ± 0.03	2.50 ± 0.06	-0.15	-6.0
Postcentral gyrus				
Postcentral gyrus (R)	2.07 ± 0.06	2.06 ± 0.19	+0.01	+0.5
Postcentral gyrus (L)	2.07 ± 0.04	2.06 ± 0.19	+0.01	+0.5
Thalamus				
Thalamus (R)	8.38 ± 0.12	8.04 ± 0.53	+0.34	+4.2
Thalamus (L)	8.15 ± 0.07	8.57 ± 0.53	-0.42	-4.9
Hippocampus				
Hippocampus (R)	4.13 ± 0.05	4.03 ± 0.41	+0.10	+2.5
Hippocampus (L)	3.86 ± 0.08	3.86 ± 0.41	+0.00	+0.0
Panel B. IGE — male, including paediatric male patients (n = 32)				
Medial temporal (R)	2.68 ± 0.06	2.78 ± 0.12	-0.10	-3.6
Medial temporal (L)	2.71 ± 0.07	2.78 ± 0.12	-0.07	-2.5
Lateral temporal – STG				
STG (R)	2.78 ± 0.03	2.82 ± 0.09	-0.04	-1.4
STG (L)	2.79 ± 0.03	2.82 ± 0.09	-0.03	-1.1
Lateral temporal – MTG				
MTG (R)	2.79 ± 0.03	2.82 ± 0.09	-0.03	-1.1
MTG (L)	2.78 ± 0.03	2.82 ± 0.09	-0.04	-1.4
Lateral temporal – ITG				
ITG (R)	2.78 ± 0.03	2.82 ± 0.09	-0.04	-1.4
ITG (L)	2.77 ± 0.03	2.82 ± 0.09	-0.05	-1.8
Lateral temporal – TTG (Heschl)				
TTG (Heschl) (R)	2.74 ± 0.04	2.82 ± 0.09	-0.08	-2.8
TTG (Heschl) (L)	2.70 ± 0.03	2.82 ± 0.09	-0.12	-4.3
Frontal lobe				
Frontal lobe (R)	2.48 ± 0.07	2.57 ± 0.12	-0.09	-3.5
Frontal lobe (L)	2.46 ± 0.07	2.57 ± 0.12	-0.11	-4.3
Parietal lobe				
Parietal lobe (R)	2.20 ± 0.08	2.25 ± 0.12	-0.05	-2.2
Parietal lobe (L)	2.20 ± 0.08	2.25 ± 0.12	-0.05	-2.2
Occipital lobe				
Occipital lobe (R)	1.78 ± 0.08	1.84 ± 0.10	-0.06	-3.3
Occipital lobe (L)	1.79 ± 0.09	1.84 ± 0.10	-0.05	-2.7

Insular cortex				
Insular cortex (R)	3.24 ± 0.21	3.05 ± 0.17	+0.19	+6.2
Insular cortex (L)	3.22 ± 0.20	3.05 ± 0.17	+0.17	+5.6
Cingulate gyrus				
Cingulate gyrus (R)	2.60 ± 0.13	2.54 ± 0.12	+0.06	+2.4
Cingulate gyrus (L)	2.60 ± 0.13	2.54 ± 0.12	+0.06	+2.4
Precentral gyrus				
Precentral gyrus (R)	2.30 ± 0.05	2.50 ± 0.05	-0.20	-8.0
Precentral gyrus (L)	2.31 ± 0.06	2.50 ± 0.06	-0.19	-7.6
Postcentral gyrus				
Postcentral gyrus (R)	2.15 ± 0.15	2.06 ± 0.19	+0.09	+4.4
Postcentral gyrus (L)	2.14 ± 0.15	2.06 ± 0.19	+0.08	+3.9
Thalamus				
Thalamus (R)	8.11 ± 0.50	8.04 ± 0.53	+0.07	+0.9
Thalamus (L)	7.87 ± 0.42	8.57 ± 0.53	-0.70	-8.2
Hippocampus				
Hippocampus (R)	4.08 ± 0.08	4.03 ± 0.41	+0.05	+1.2
Hippocampus (L)	3.89 ± 0.10	3.86 ± 0.41	+0.03	+0.8
Panel C. IGE — female, including paediatric female patients (n = 28)				
Medial temporal (R)	2.67 ± 0.12	2.78 ± 0.12	-0.11	-4.0
Medial temporal (L)	2.71 ± 0.11	2.78 ± 0.12	-0.07	-2.5
Lateral temporal – STG				
STG (R)	2.77 ± 0.08	2.82 ± 0.09	-0.05	-1.8
STG (L)	2.79 ± 0.06	2.82 ± 0.09	-0.03	-1.1
Lateral temporal – MTG				
MTG (R)	2.77 ± 0.08	2.82 ± 0.09	-0.05	-1.8
MTG (L)	2.78 ± 0.07	2.82 ± 0.09	-0.04	-1.4
Lateral temporal – ITG				
ITG (R)	2.78 ± 0.05	2.82 ± 0.09	-0.04	-1.4
ITG (L)	2.77 ± 0.03	2.82 ± 0.09	-0.05	-1.8
Lateral temporal – TTG (Heschl)				
TTG (Heschl) (R)	2.74 ± 0.04	2.82 ± 0.09	-0.08	-2.8
TTG (Heschl) (L)	2.74 ± 0.04	2.82 ± 0.09	-0.08	-2.8
Frontal lobe				
Frontal lobe (R)	2.56 ± 0.05	2.57 ± 0.12	-0.01	-0.4
Frontal lobe (L)	2.45 ± 0.04	2.57 ± 0.12	-0.12	-4.7
Parietal lobe				
Parietal lobe (R)	2.17 ± 0.07	2.25 ± 0.12	-0.08	-3.6
Parietal lobe (L)	2.17 ± 0.07	2.25 ± 0.12	-0.08	-3.6
Occipital lobe				
Occipital lobe (R)	1.77 ± 0.02	1.84 ± 0.10	-0.07	-3.8
Occipital lobe (L)	1.77 ± 0.04	1.84 ± 0.10	-0.07	-3.8
Insular cortex				
Insular cortex (R)	3.30 ± 0.22	3.05 ± 0.17	+0.25	+8.2
Insular cortex (L)	3.28 ± 0.15	3.05 ± 0.17	+0.23	+7.5
Cingulate gyrus				
Cingulate gyrus (R)	2.51 ± 0.04	2.54 ± 0.12	-0.03	-1.2
Cingulate gyrus (L)	2.55 ± 0.04	2.54 ± 0.12	+0.01	+0.4
Precentral gyrus				
Precentral gyrus (R)	2.29 ± 0.03	2.50 ± 0.05	-0.21	-8.4
Precentral gyrus (L)	2.30 ± 0.04	2.50 ± 0.06	-0.20	-8.0
Postcentral gyrus				
Postcentral gyrus (R)	2.26 ± 0.13	2.06 ± 0.19	+0.20	+9.7
Postcentral gyrus (L)	2.26 ± 0.13	2.06 ± 0.19	+0.20	+9.7
Thalamus				
Thalamus (R)	7.90 ± 0.29	8.04 ± 0.53	-0.14	-1.7

Thalamus (L)	7.87 ± 0.42	8.57 ± 0.53	-0.70	-8.2
Hippocampus				
Hippocampus (R)	4.08 ± 0.35	4.03 ± 0.41	+0.05	+1.2
Hippocampus (L)	3.87 ± 0.28	3.86 ± 0.41	+0.01	+0.3

3.4 MTLE groups — right- and left-sided disease

Right MTLE (n = 11). The largest reference-based deviation was ipsilateral hippocampal volume reduction: the mean right hippocampal volume was 3.45 ± 0.04 compared with 4.03 ± 0.41 (−14.4%); the left hippocampal deviation was −0.8% (Table 4, Panel A). Left thalamic volume differed by −9.9%, compared with +0.5% on the right. Precentral thickness was below the reference means on both sides (−9.6% each), as was transverse temporal thickness (−6.4% bilaterally). Additional negative deviations involved right superior and middle temporal gyri (−4.3% and −5.0%) and right frontal cortex (−6.6%). Insular, postcentral and left parietal measurements were above the corresponding references. Inferences regarding the population distribution or clinical significance of these deviations are limited by the subgroup size.

Left MTLE (n = 9). The largest negative reference-based deviation involved the left hippocampus (mean 3.32 ± 0.08 vs reference 3.86 ± 0.41; −14.0%), while the right hippocampal deviation was +2.2% (Table 4, Panel B). Left thalamic volume differed by −10.2%, with a +0.1% difference on the right. Bilateral precentral cortical thickness was below the reference means (−10.4% right, −10.8% left), as was transverse temporal thickness (−6.9% right, −6.4% left). Left superior and middle temporal gyri showed negative differences (−4.6% and −5.0%). Positive deviations were seen in the bilateral insula (+4.6% right, +3.6% left), left parietal cortex (+5.3%) and postcentral gyri (+1.9% each). These estimates are exploratory given the small number of participants.

Table 4. Cortical thickness and subcortical volume summaries in MTLE. Panel A: right-sided MTLE (n = 11); Panel B: left-sided MTLE (n = 9). Percentage deviations compare each subgroup mean with a fixed reference mean rather than a matched control cohort. Negative values are below, and positive values are above, the corresponding reference mean.

Region	Patient value (mean ± SD)	Reference value (mean ± SD)	Difference	Deviation (%)
Panel A. MTLE — right-sided seizure onset (n = 11)				
Medial temporal (R)	2.71 ± 0.08	2.78 ± 0.12	-0.07	-2.5
Medial temporal (L)	2.80 ± 0.04	2.78 ± 0.12	+0.02	+0.7
Lateral temporal – STG				
STG (R)	2.70 ± 0.03	2.82 ± 0.09	-0.12	-4.3
STG (L)	2.81 ± 0.03	2.82 ± 0.09	-0.01	-0.4
Lateral temporal – MTG				
MTG (R)	2.68 ± 0.02	2.82 ± 0.09	-0.14	-5.0
MTG (L)	2.80 ± 0.03	2.82 ± 0.09	-0.02	-0.7
Lateral temporal – ITG				
ITG (R)	2.79 ± 0.02	2.82 ± 0.09	-0.03	-1.1
ITG (L)	2.80 ± 0.03	2.82 ± 0.09	-0.02	-0.7
Lateral temporal – TTG (Heschl)				
TTG (Heschl) (R)	2.64 ± 0.03	2.82 ± 0.09	-0.18	-6.4
TTG (Heschl) (L)	2.64 ± 0.04	2.82 ± 0.09	-0.18	-6.4
Frontal lobe				
Frontal lobe (R)	2.40 ± 0.04	2.57 ± 0.12	-0.17	-6.6
Frontal lobe (L)	2.47 ± 0.08	2.57 ± 0.12	-0.10	-3.9
Parietal lobe				
Parietal lobe (R)	2.28 ± 0.03	2.25 ± 0.12	+0.03	+1.3
Parietal lobe (L)	2.32 ± 0.02	2.25 ± 0.12	+0.07	+3.1
Occipital lobe				
Occipital lobe (R)	1.87 ± 0.03	1.84 ± 0.10	+0.03	+1.6

Occipital lobe (L)	1.86 ± 0.03	1.84 ± 0.10	+0.02	+1.1
Insular cortex				
Insular cortex (R)	3.13 ± 0.14	3.05 ± 0.17	+0.08	+2.6
Insular cortex (L)	3.11 ± 0.09	3.05 ± 0.17	+0.06	+2.0
Cingulate gyrus				
Cingulate gyrus (R)	2.54 ± 0.10	2.54 ± 0.12	+0.00	+0.0
Cingulate gyrus (L)	2.55 ± 0.03	2.54 ± 0.12	+0.01	+0.4
Precentral gyrus				
Precentral gyrus (R)	2.26 ± 0.03	2.50 ± 0.05	-0.24	-9.6
Precentral gyrus (L)	2.26 ± 0.03	2.50 ± 0.06	-0.24	-9.6
Postcentral gyrus				
Postcentral gyrus (R)	2.18 ± 0.06	2.06 ± 0.19	+0.12	+5.8
Postcentral gyrus (L)	2.13 ± 0.04	2.06 ± 0.19	+0.07	+3.4
Thalamus				
Thalamus (R)	8.08 ± 0.12	8.04 ± 0.53	+0.04	+0.5
Thalamus (L)	7.72 ± 0.06	8.57 ± 0.53	-0.85	-9.9
Hippocampus				
Hippocampus (R)	3.45 ± 0.04	4.03 ± 0.41	-0.58	-14.4
Hippocampus (L)	3.83 ± 0.08	3.86 ± 0.41	-0.03	-0.8
Panel B. MTLE — left-sided seizure onset (n = 9)				
Medial temporal (R)	2.80 ± 0.08	2.78 ± 0.12	+0.02	+0.7
Medial temporal (L)	2.76 ± 0.04	2.78 ± 0.12	-0.02	-0.7
Lateral temporal – STG				
STG (R)	2.84 ± 0.03	2.82 ± 0.09	+0.02	+0.7
STG (L)	2.69 ± 0.03	2.82 ± 0.09	-0.13	-4.6
Lateral temporal – MTG				
MTG (R)	2.81 ± 0.02	2.82 ± 0.09	-0.01	-0.4
MTG (L)	2.68 ± 0.03	2.82 ± 0.09	-0.14	-5.0
Lateral temporal – ITG				
ITG (R)	2.83 ± 0.02	2.82 ± 0.09	+0.01	+0.4
ITG (L)	2.81 ± 0.03	2.82 ± 0.09	-0.01	-0.4
Lateral temporal – TTG (Heschl)				
TTG (Heschl) (R)	2.63 ± 0.03	2.82 ± 0.09	-0.19	-6.9
TTG (Heschl) (L)	2.64 ± 0.04	2.82 ± 0.09	-0.18	-6.4
Frontal lobe				
Frontal lobe (R)	2.45 ± 0.04	2.57 ± 0.12	-0.12	-4.7
Frontal lobe (L)	2.46 ± 0.08	2.57 ± 0.12	-0.11	-4.3
Parietal lobe				
Parietal lobe (R)	2.28 ± 0.03	2.25 ± 0.12	+0.03	+1.3
Parietal lobe (L)	2.37 ± 0.02	2.25 ± 0.12	+0.12	+5.3
Occipital lobe				
Occipital lobe (R)	1.80 ± 0.03	1.84 ± 0.10	-0.04	-2.2
Occipital lobe (L)	1.86 ± 0.03	1.84 ± 0.10	+0.02	+1.1
Insular cortex				
Insular cortex (R)	3.19 ± 0.14	3.05 ± 0.17	+0.14	+4.6
Insular cortex (L)	3.16 ± 0.09	3.05 ± 0.17	+0.11	+3.6
Cingulate gyrus				
Cingulate gyrus (R)	2.54 ± 0.10	2.54 ± 0.12	+0.00	+0.0
Cingulate gyrus (L)	2.56 ± 0.03	2.54 ± 0.12	+0.02	+0.8
Precentral gyrus				
Precentral gyrus (R)	2.24 ± 0.03	2.50 ± 0.05	-0.26	-10.4
Precentral gyrus (L)	2.23 ± 0.03	2.50 ± 0.06	-0.27	-10.8
Postcentral gyrus				
Postcentral gyrus (R)	2.10 ± 0.06	2.06 ± 0.19	+0.04	+1.9
Postcentral gyrus (L)	2.10 ± 0.04	2.06 ± 0.19	+0.04	+1.9
Thalamus				

Thalamus (R)	8.05 ± 0.12	8.04 ± 0.53	+0.01	+0.1
Thalamus (L)	7.70 ± 0.06	8.57 ± 0.53	-0.87	-10.2
Hippocampus				
Hippocampus (R)	4.12 ± 0.04	4.03 ± 0.41	+0.09	+2.2
Hippocampus (L)	3.32 ± 0.08	3.86 ± 0.41	-0.54	-14.0

3.5 Cross-group description: recurring and subgroup-associated patterns

Figure 2 displays reference-based percentage deviations across 28 anatomical measures and five analytic subgroups. Table 5 ranks the six largest absolute deviations for each subgroup. Three descriptive patterns were apparent; these rankings do not represent formal comparisons between independent groups.

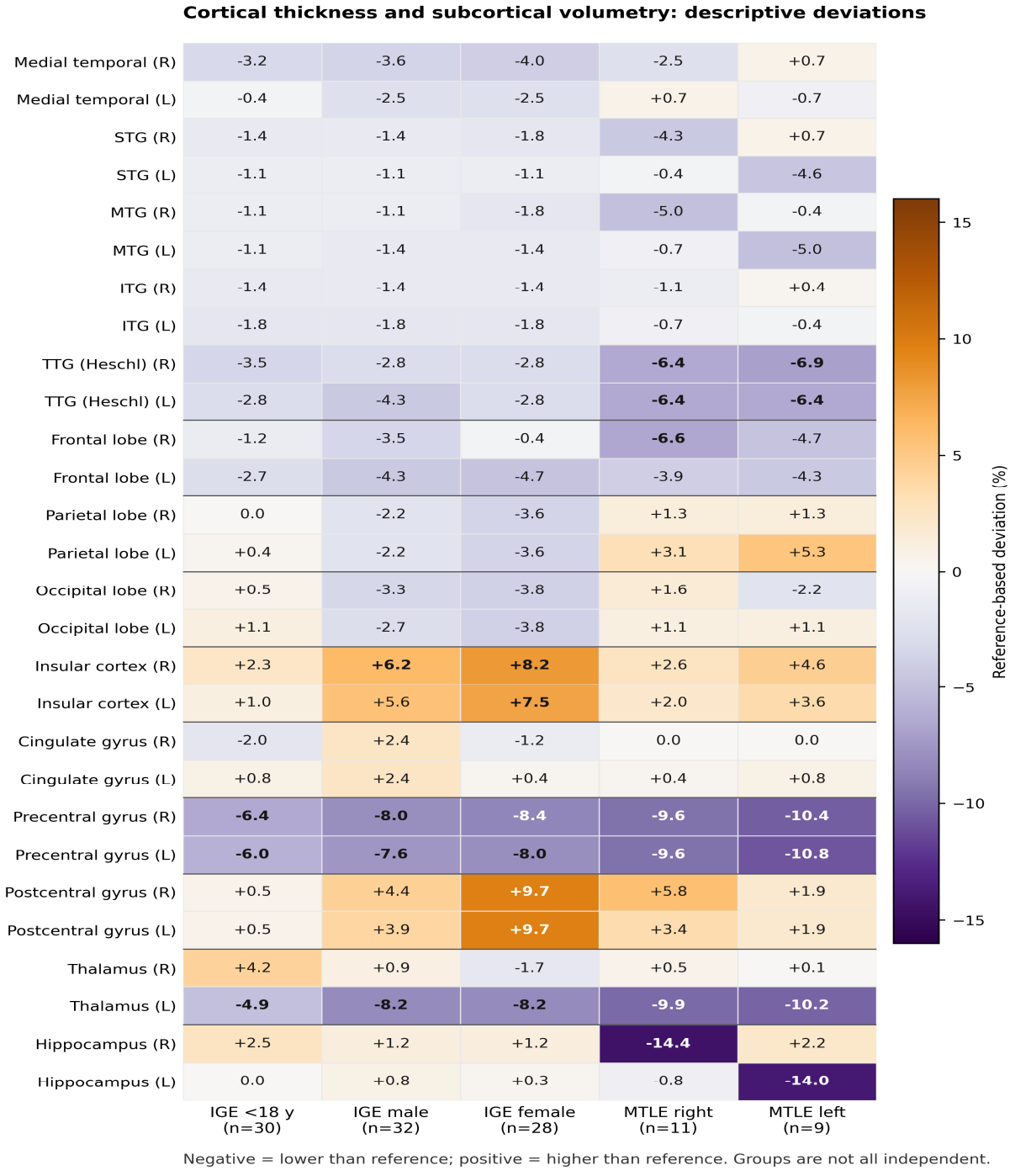


Figure 2. Reference-based percentage deviations for 28 regional cortical and subcortical measures (rows) across five analytic subgroups (columns). The colour-blind-accessible purple–orange scale is

centred on zero; each cell also displays its numerical value. Negative values indicate lower, and positive values higher, subgroup means relative to fixed reference means. Bilateral precentral and left-thalamic deviations were negative in all displayed subgroups. The paediatric and sex-defined IGE groups overlap.

Pattern 1 recurring descriptive differences. Negative percentage deviations for bilateral precentral cortical thickness and left thalamic volume were recorded in all five subgroup summaries (Figure 3a). The precentral deviations ranged from −6.0% to −10.8%, and the left thalamic deviations from −4.9% to −10.2%. Right thalamic deviations were smaller (−1.7% to +0.9%) in the two MTLE and sex-defined IGE groups and were +4.2% in paediatric IGE. The recurrence of these directional findings warrants controlled validation but does not establish a statistically confirmed common biomarker.

Pattern 2 MTLE-associated deviations. Both MTLE groups showed large negative ipsilateral hippocampal deviations (−14.4% in right MTLE and −14.0% in left MTLE) and negative bilateral transverse temporal (Heschl) cortical differences (−6.4% to −6.9%) (Figure 3b). The transverse temporal deviations were smaller in the IGE subgroup summaries (−2.8% to −4.3%). Negative superior and middle temporal deviations (approximately −4.3% to −5.0%) were also present ipsilateral to the MTLE focus. These were descriptive contrasts rather than statistically tested syndrome effects.

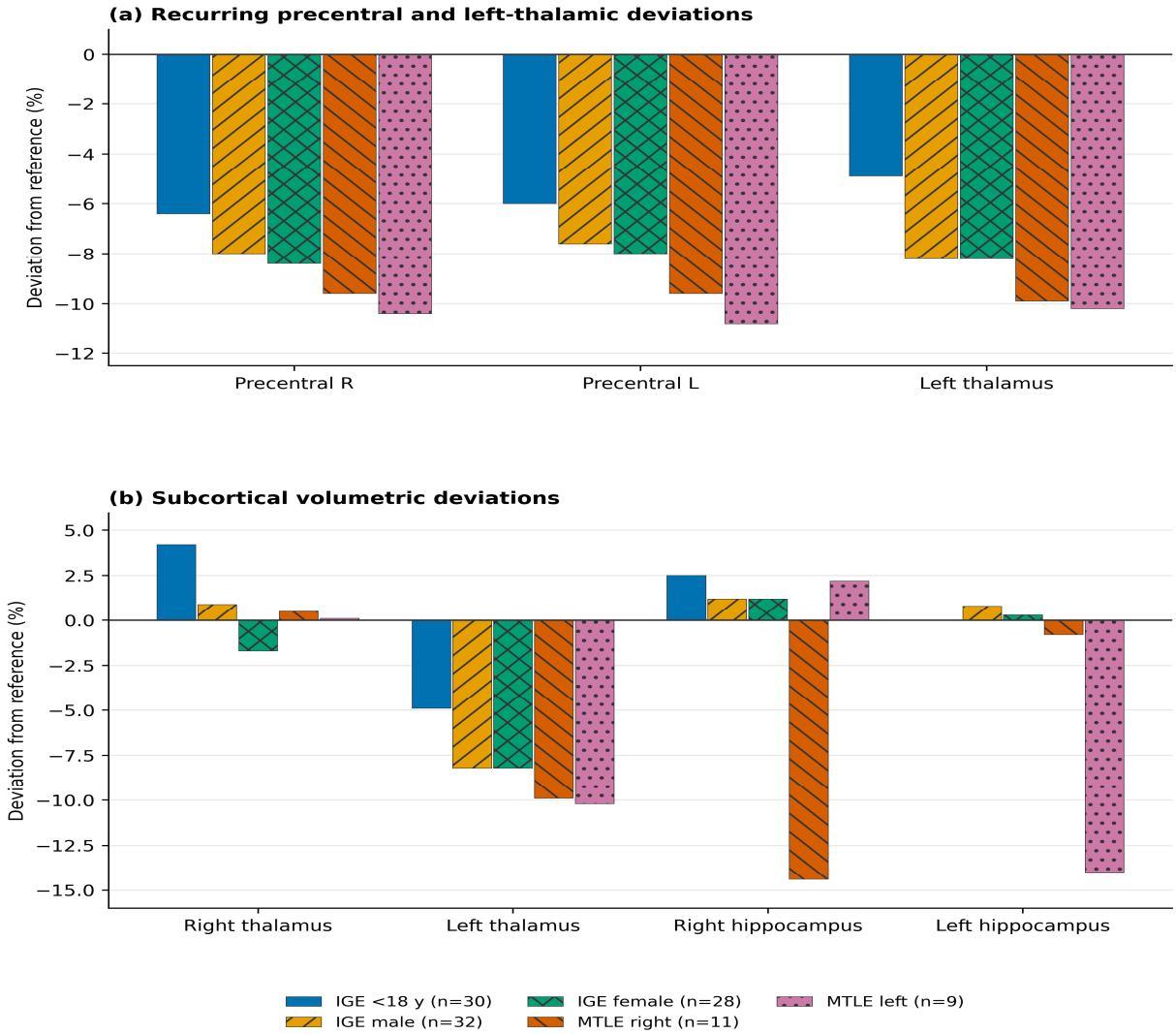


Figure 3. Reference-based deviations in five analytic subgroups. (a) Precentral cortical thickness (right and left) and left thalamic volume; negative deviations are observed in each subgroup. (b) Right and left thalamic and hippocampal volumes; the largest negative hippocampal deviations occur ipsilateral to the affected temporal lobe in MTLE. Colours and bar hatching distinguish subgroups;

values represent descriptive comparisons with fixed region-specific reference means. IGE paediatric and sex-defined groups overlap.

Pattern 3 IGE sex-defined summaries. Positive insular and postcentral deviations were numerically larger in the female-defined IGE subgroup (+8.2% right insula and +9.7% bilateral postcentral cortex) than in the male-defined subgroup (+6.2% right insula and +4.4% right postcentral cortex). Bilateral cingulate deviations were +2.4% in the male-defined subgroup. Because the sex-defined groups included paediatric participants and no age-adjusted comparisons were performed, the observed differences should not be interpreted as established sex effects. The MTLE groups generally showed larger precentral deviations than the overlapping IGE summaries (Figure 3a).

Table 5. Six largest regional deviations from normative reference values in each analytic group, ranked by absolute percentage deviation. R: right; L: left; STG/MTG/ITG: superior/middle/inferior temporal gyrus; TTG: transverse temporal (Heschl) gyrus.

Rank	IGE <18 y	IGE male	IGE female	MTLE right	MTLE left
1	Precentral gyrus (R), −6.4%	Thalamus (L), −8.2%	Postcentral gyrus (R), +9.7%	Hippocampus (R), −14.4%	Hippocampus (L), −14.0%
2	Precentral gyrus (L), −6.0%	Precentral gyrus (R), −8.0%	Postcentral gyrus (L), +9.7%	Thalamus (L), −9.9%	Precentral gyrus (L), −10.8%
3	Thalamus (L), −4.9%	Precentral gyrus (L), −7.6%	Precentral gyrus (R), −8.4%	Precentral gyrus (R), −9.6%	Precentral gyrus (R), −10.4%
4	Thalamus (R), +4.2%	Insular cortex (R), +6.2%	Insular cortex (R), +8.2%	Precentral gyrus (L), −9.6%	Thalamus (L), −10.2%
5	TTG (Heschl) (R), −3.5%	Insular cortex (L), +5.6%	Thalamus (L), −8.2%	Frontal lobe (R), −6.6%	TTG (Heschl) (R), −6.9%
6	Medial temporal (R), −3.2%	Postcentral gyrus (R), +4.4%	Precentral gyrus (L), −8.0%	TTG (Heschl) (R), −6.4%	TTG (Heschl) (L), −6.4%

4. Discussion

4.1 Principal findings

In this retrospective 1.5 T MRI cohort, the reported CAT12-based group summaries showed negative reference-based deviations in bilateral precentral thickness and left thalamic volume across IGE and MTLE clinical strata. Ipsilateral hippocampal and transverse temporal differences were more prominent within the small MTLE groups, while insular and postcentral positive deviations were apparent in IGE sex-defined summaries. These findings represent an exploratory anatomical description rather than confirmation of a reproducible thalamocortical signature or evidence of independent syndrome- or sex-related effects.

The principal methodological observation is that the regions could be quantified using an automated workflow from 1.5 T examinations. However, technical feasibility is distinct from diagnostic validity. Reference-based percentage deviations without a contemporaneous, locally matched control group cannot establish whether individual patients have abnormal brain structure. In addition, the right-thalamic predominance described by the ENIGMA case-control analysis [7] differs from the left-thalamic predominance in the present subgroup summaries; agreement is therefore limited to selected anatomic domains rather than a complete replication.

4.2 The precentral gyrus as a convergent node

Bilateral precentral cortical thickness showed negative percentage deviations in each subgroup summary, with reported values ranging from −6.0% to −10.8%. The precentral gyrus contains the primary motor cortex and is relevant to seizure propagation through distributed motor networks. The ENIGMA-Epilepsy analysis also identified bilateral precentral thinning across common epilepsy groups and associations with epilepsy duration [7]. The present reference-based results are anatomically compatible with this cortical observation, but no within-cohort association with epilepsy duration or adjustment for subgroup composition was evaluated. The

numerical variation across the overlapping strata should not be interpreted as a progression gradient.

Multiple explanations could account for regional cortical thickness differences in epilepsy, including developmental factors, recurrent seizure activity, medication exposure, comorbidity and measurement-related variability. The available cross-sectional measurements cannot distinguish among these possibilities. In particular, age-related cortical maturation and reference-population differences are relevant to the paediatric group; conclusions regarding seizure type or disease progression would require adequately characterized, non-overlapping cohorts with repeated imaging.

4.3 The thalamus as the shared hub

Left thalamic volume differed negatively from the selected reference mean in every subgroup (−4.9% to −10.2%). The thalamus participates in distributed cortico-subcortical pathways involved in focal and generalized seizures. Previous volumetric and morphometric studies have described thalamic abnormalities in generalized and focal epilepsies [12–14], consistent with the broader system-epilepsies framework [15]. Nevertheless, these descriptive percentage deviations do not determine whether thalamic differences preceded seizures, developed during the clinical course or reflect differences between the reference and clinical populations.

A left-sided predominance was observed in the group summaries, whereas ENIGMA-Epilepsy reported a predominantly right-sided thalamic reduction relative to matched controls [7]. This difference may arise from cohort composition, reference-value selection, hemispheric segmentation, acquisition characteristics or biological heterogeneity. The functional thalamic network study by He and colleagues associated presurgical connectivity features with postoperative outcomes [20]; its functional measures cannot be taken as validation of the left-thalamic volumetric differences observed here. No structural connectivity or language-dominance assessment was performed.

The positive right-thalamic deviation in paediatric IGE (+4.2%) occurred alongside a negative left-thalamic deviation (−4.9%). Without age- and sex-matched controls, this asymmetry cannot be attributed to compensatory plasticity or a developmental disease stage. Repeat imaging and appropriately matched reference groups would be required to determine its reproducibility and clinical relevance.

4.4 Insular and postcentral thickening: an autonomic somatosensory overlay

Positive deviations in insular and postcentral thickness were observed in several subgroup summaries, with the largest values in the female-defined IGE group (+8.2% for right insula and +9.7% for bilateral postcentral cortex). Ogren and colleagues reported regional cortical thickness differences involving the insula, cingulate and postcentral gyri in generalized tonic–clonic seizures, with variation by sex and hemisphere [17]. These regions contribute to interoceptive, sensory and autonomic processing [18]. Such anatomical relationships justify further investigation but do not establish an autonomic mechanism in this cohort.

Increased apparent cortical thickness may have several explanations, including biological differences, variation in grey–white matter contrast, tissue segmentation effects or reference-population mismatch. The reported differences cannot distinguish among these possibilities, and the sex-defined summaries were not adjusted for age or other relevant variables. Accordingly, the anatomical associations are best regarded as exploratory and require replication with standardized acquisition, quality control and independent control data.

Structural imaging abnormalities in autonomic and subcortical regions have been investigated in relation to sudden unexpected death in epilepsy (SUDEP) [19]. However, autonomic function, peri-ictal cardiorespiratory events and SUDEP outcomes were not assessed in this cohort. The present insular, cingulate and thalamic measurements cannot be used to estimate individual SUDEP risk or guide counselling, and any prognostic application would require prospective validation.

4.5 Laterality and extrahippocampal injury in MTLE

Both MTLE groups showed negative reference-based deviations in the ipsilateral hippocampus (−14.4% in right MTLE; −14.0% in left MTLE), while contralateral hippocampal means were close to the corresponding reference values. Negative deviations in bilateral precentral and transverse temporal thickness and left thalamic volume were also present. Descriptive differences between right and left MTLE included ipsilateral superior and middle temporal cortical measures, a larger positive left parietal deviation in left MTLE (+5.3% vs +3.1%) and differences in the magnitude of insular deviations. Previous investigations have reported laterality-associated structural and network characteristics in MTLE [8,9]. Given the small sample sizes and absence of matched controls, the present differences should not be regarded as verified laterality effects.

Transverse temporal (Heschl) cortical thickness was below the reference mean bilaterally in both MTLE groups (−6.4% to −6.9%), compared with smaller negative deviations in IGE (−2.8% to −4.3%). As Heschl gyrus is involved in auditory processing and lies within broader temporal networks, this descriptive observation merits examination in larger, controlled investigations. No auditory assessment or postoperative outcome measure was available to determine its functional or presurgical significance.

4.6 Comparison with ENIGMA-Epilepsy

The ENIGMA-Epilepsy consortium identified bilateral precentral cortical thinning and predominantly right-sided thalamic volume reduction across epilepsy groups when compared with matched healthy controls [7]. Bilateral precentral negative deviations in the present analysis are directionally compatible with that report, whereas the left-predominant thalamic findings are not an exact anatomical replication. Moreover, ENIGMA effect sizes (Cohen's d) represent adjusted case-control contrasts, whereas the current percentages compare rounded subgroup means with fixed external reference means. They are not directly comparable. Small and overlapping strata, unmeasured confounding, and differences in scanner, segmentation and reference population may also affect observed patterns. Thus, the external literature supports further investigation of thalamocortical involvement but cannot validate the magnitude, laterality or clinical significance of these descriptive estimates.

4.7 Clinical implications

Several research implications follow. First, automated cortical and subcortical measurement from 1.5 T datasets was achievable in the evaluated clinical cohort, supporting the feasibility of further methodological studies. Second, the precentral cortex and thalamus are reasonable a priori regions for comparison against age-, sex- and scanner-matched controls in larger samples. Third, insular and postcentral differences could be explored alongside autonomic measures, while hippocampal and extrahippocampal estimates in MTLE could be studied in relation to seizure localization and long-term outcomes. Although prior work has investigated SUDEP-associated imaging patterns [19] and presurgical thalamic connectivity [20], neither SUDEP prediction nor surgical outcome prediction was tested here. Quantitative measurements should therefore complement, not replace, standard clinical MRI interpretation and epilepsy assessment.

4.8 Limitations and future directions

This study was limited by its retrospective, cross-sectional, single-centre design and the small right- and left-MTLE groups (n = 11 and n = 9). The paediatric IGE stratum overlapped with sex-defined strata, precluding independent age-by-sex inference; no adjusted comparison tested these subgroup differences. A major limitation was the absence of an in-house healthy control cohort. The same region-specific comparator mean was used across all subgroups, without individual matching for age, sex, local ancestry, scanner or acquisition protocol. These differences could alter both the magnitude and direction of the reported percentages and prevent the deviations from being interpreted as standardized normative scores. Participant-level measurements and full provenance of the reference distributions were unavailable for

verification of inferential uncertainty. Several reported cortical thickness SDs were small (for example, 0.03 mm); rounding, segmentation-related features and underlying dispersion should be examined using the individual CAT12 outputs before drawing conclusions about biological variability. Medication exposure, seizure frequency, disease duration, illness severity, MRI-negative status, language dominance and SUDEP-related outcomes could not be evaluated as covariates or endpoints. Single-pipeline processing and imaging at 1.5 T introduce additional measurement and reproducibility limitations. Consequently, the observed patterns are hypothesis-generating and cannot support patient-level diagnosis, risk stratification, prediction or causal inference.

Future studies should include independent, non-overlapping epilepsy cohorts and locally recruited healthy participants matched for age and sex, scanned with harmonized 1.5 T and/or 3 T protocols. Prespecified quality-control procedures, region-level raw measurements, appropriate uncertainty estimates and multiplicity-aware analyses would help establish reproducibility. Longitudinal imaging and assessment of seizure burden, medication exposure, autonomic physiology and surgical outcomes could then determine whether regional morphometry has clinical prognostic value.

5. Conclusion

In this retrospective 1.5 T MRI cohort, negative reference-based deviations in bilateral precentral cortical thickness and left thalamic volume were observed across the IGE and MTLE subgroup summaries. Ipsilateral hippocampal deviations were particularly prominent in MTLE, whereas insular and postcentral measurements differed between the overlapping IGE sex-defined strata. These descriptive findings are hypothesis-generating. Small subgroup sizes, overlapping IGE samples, lack of locally matched healthy controls and uncertainty about reference-population comparability preclude confirmation of a common disease-specific structural signature or any immediate diagnostic or prognostic application. Independent, controlled and longitudinal studies are warranted.

Declarations

Ethics approval and consent to participate: The study was approved by the institutional ethics committee, which waived individual informed consent for this fully anonymized retrospective analysis. All procedures followed applicable institutional and national requirements.

Consent for publication: Not applicable; no identifiable patient data are presented.

Availability of data and materials: The anonymized datasets analysed during the current study are available from the corresponding author on reasonable request.

Competing interests: The authors declare that they have no competing interests.

Funding: This research received no specific grant from any funding agency in the public, commercial or not-for-profit sectors.

Authors' contributions: Archit Tyagi and Shino Shajan contributed to interpretation of the imaging findings and critical revision of the article. Both authors reviewed and approved the final version.

Acknowledgements: The authors thank the staff of the radiology department for database support.

References

1. Fisher RS, Acevedo C, Arzimanoglou A, et al. ILAE official report: a practical clinical definition of epilepsy. Epilepsia. 2014;55(4):475–482.
2. Bell GS, Neligan A, Sander JW. An unknown quantity—the worldwide prevalence of epilepsy. Epilepsia. 2014;55(7):958–962.
3. French JA. Refractory epilepsy: clinical overview. Epilepsia. 2007;48(Suppl 1):3–7.
4. Bernhardt BC, Bonilha L, Gross DW. Network analysis for a network disorder: the emerging role of graph theory in the study of epilepsy. Epilepsy Behav. 2015;50:162–170.
5. Vaughan DN, Rayner G, Tailby C, Jackson GD. MRI-negative temporal lobe epilepsy: a

network disorder of neocortical connectivity. Neurology. 2016;87(18):1934–1942.
6. Blümcke I, Thom M, Aronica E, et al. International consensus classification of hippocampal sclerosis in temporal lobe epilepsy: a task force report from the ILAE Commission on Diagnostic Methods. Epilepsia. 2013;54(7):1315–1329.
7. Whelan CD, Altmann A, Botía JA, et al. Structural brain abnormalities in the common epilepsies assessed in a worldwide ENIGMA study. Brain. 2018;141(2):391–408. doi:10.1093/brain/awx341.
8. Liu M, Bernhardt BC, Bernasconi A, Bernasconi N. Gray matter structural compromise is equally distributed in left and right temporal lobe epilepsy. Hum Brain Mapp. 2016;37(2):515–524.
9. de Campos BM, Coan AC, Yasuda CL, Casseb RF, Cendes F. Large-scale brain networks are distinctly affected in right and left mesial temporal lobe epilepsy. Hum Brain Mapp. 2016;37(9):3137–3152.
10. Woermann FG, Sisodiya SM, Free SL, Duncan JS. Quantitative MRI in patients with idiopathic generalized epilepsy: evidence of widespread cerebral structural changes. Brain. 1998;121(Pt 9):1661–1667.
11. Betting LE, Mory SB, Lopes-Cendes I, et al. MRI reveals structural abnormalities in patients with idiopathic generalized epilepsy. Neurology. 2006;67(5):848–852.
12. Natsume J, Bernasconi N, Andermann F, Bernasconi A. MRI volumetry of the thalamus in temporal, extratemporal, and idiopathic generalized epilepsy. Neurology. 2003;60(8):1296–1300.
13. Du H, Zhang Y, Xie B, et al. Regional atrophy of the basal ganglia and thalamus in idiopathic generalized epilepsy. J Magn Reson Imaging. 2011;33(4):817–821.
14. Bernhardt BC, Rozen DA, Worsley KJ, Evans AC, Bernasconi N, Bernasconi A. Thalamo-cortical network pathology in idiopathic generalized epilepsy: insights from MRI-based morphometric correlation analysis. Neuroimage. 2009;46(2):373–381.
15. Avanzini G, Manganotti P, Meletti S, et al. The system epilepsies: a pathophysiological hypothesis. Epilepsia. 2012;53(5):771–778.
16. Desikan RS, Ségonne F, Fischl B, et al. An automated labeling system for subdividing the human cerebral cortex on MRI scans into gyral based regions of interest. Neuroimage. 2006;31(3):968–980.
17. Ogren JA, Tripathi R, Macey PM, Kumar R, Stern JM, Eliashiv DS, et al. Regional cortical thickness changes accompanying generalized tonic-clonic seizures. Neuroimage Clin. 2018;20:205–215. doi:10.1016/j.nicl.2018.07.015.
18. Kimmerly DS, O'Leary DD, Menon RS, Gati JS, Shoemaker JK. Cortical regions associated with autonomic cardiovascular regulation during lower body negative pressure in humans. J Physiol. 2005;569(Pt 1):331–345.
19. Wandschneider B, Koepp M, Scott C, et al. Structural imaging biomarkers of sudden unexpected death in epilepsy. Brain. 2015;138(10):2907–2919. doi:10.1093/brain/awv233.
20. He X, Doucet GE, Pustina D, Sperling MR, Sharan AD, Tracy JI. Presurgical thalamic "hubness" predicts surgical outcome in temporal lobe epilepsy. Neurology. 2017;88(24):2285–2293. doi:10.1212/WNL.0000000000004035.